Numerical Evaluation of the Radar Cross Section of Human Breathing Models

Marta Cavagnaro, Erika Pittella, and Stefano Pisa

Dept. of Information Engineering, Electronics and Telecommunications (DIET)
Sapienza University of Rome, Rome, Italy
[cavagnaro, pittella, pisa]@diet.uniroma1.it

Abstract ─ In this paper, anatomical models of the human body are used to evaluate the radar cross section (RCS) of breathing subjects. The study is performed by using a self-developed finite difference time domain (FDTD) code implemented in the message passing interface environment (MPI). The realized models represent three different phases of the breathing activity taking into account the respiration physiology and the pulmonary mechanics. In particular, the end expiration phase (resting state), the end of a normal inspiration phase (tidal), and the end of a deep inspiration phase (deep) were considered. Computed results show RCS values of the resting state model in agreement with literature data, and appreciable variations of the RCS determined by the breathing activity. Simulations performed with homogeneous body models suggest that these differences depend both on the model anatomy and on the tissue dielectric properties.

Index Terms ─ Breathing models, electromagnetic scattering, radar cross section.

I. INTRODUCTION

Ultra-wide band (UWB) radars for remote sensing of vital signs, as the breath and cardiac activity, can be useful for monitoring the breathing of patients during hospital confinement, for through-the-wall sensing, and for the rescue of people under rubbles or snow. UWB radars detect the time of arrival and the amplitude variations of UWB pulses once reflected by the human body to evaluate the thorax and heart movements, and then derive the cardio-respiratory activities [1]. The knowledge of the radar cross section (RCS) of men in correspondence of different respiration phases is of great importance for the design of UWB radars for remote monitoring of respiratory activity. In particular, the RCS is essential in predicting the time behavior of the radar-received signal, thus helping designing stand-alone apparatuses [1].

In literature, few works deal with the RCS of the human body including experimental investigations [2]-[5] and recent numerical studies [1], [6]-[7]. These works indicate RCS absolute values of the order of 1 m^2, with large fluctuations with the frequency. However, these limited data are based on man models at rest and they do not consider variations of the tissue properties with frequency.

In this paper, a finite-difference time-domain (FDTD) parallel code was used to evaluate the RCS of anatomical models of the human body as a function of the frequency. Models of men in resting state and previously developed models representing a tidal breath and a deep breath were considered [8], [9]. The RCS was evaluated in a frequency range between 1 and 9 GHz with 1 GHz step, taking into account the frequency behavior of the tissues' dielectric parameters and the variations of the lung geometry and dielectric parameters with the respiration.

II. METHODS AND MODELS

A. FDTD method

The RCS was computed by using a parallel self-developed code based on the FDTD method and implemented in the MPI environment [10]. Figure 1 shows the simulated geometry: a plane wave with sinusoidal time dependence propagating along the y-axis impinges on the human body (front-back of the body model) with the electric field linearly polarized along the z-axis (height of the body model). To excite the plane wave, the code divides the whole volume under study in a total-field and a scattered-field region by means of a Huygens' surface [11], [12]. The scattered-field region is closed by applying a uniaxial perfectly matched layer (UPML) absorbing boundary condition made by a 5-cell layer with parabolic profile and a 0.01% nominal reflection coefficient. At steady state, the scattered electric field values obtained on a surface surrounding the human body were stored and used to evaluate the RCS of the considered body model by way of a near-far field transformation.

Submitted On: January 28, 2015
Accepted On: November 8, 2015

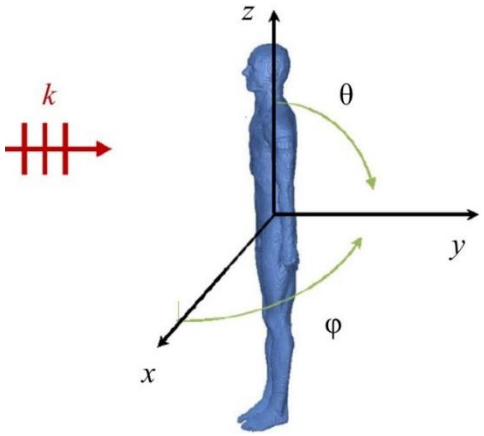

Fig. 1. Simulated geometry: the human body anatomical model faces the plane wave propagating towards the positive y-axis with a linear vertical polarization (i.e., the electric field is aligned with the z-axis).

B. Human anatomical models

Two different anatomical models were considered: the Visible Human [13] (VH) and Duke of the Virtual Family [14]. In particular, the VH was used for validation purposes, while the Duke, representing a model closer to the standard man than the VH, was used to study the RCS as a function of the breathing activity. To this end, it is worth mentioning that the body models usually considered in dosimetry studies represent resting state bodies (RS); i.e., a body at the end of the respiration phase, when little air is present into the lungs.

To take into account the breathing activity, in [8] two models were developed considering the respiration physiology and the pulmonary mechanics [15]. In brief, starting from the RS Duke model, constituted by a three-dimensional matrix of integer numbers representing 77 different tissues, lung cells were added simulating both a diaphragm displacement and an enlargement of the rib cage.

Changing the entity of the diaphragm displacement and of the rib cage enlargement, two respiration phases were obtained: the tidal breath (TB), corresponding to a state of normal inspiration with an inhaled volume of air equal to about 500 cm^3 [15], and the deep breath (DB), corresponding to a state in which a high volume of air, approximately 860 cm^3, is inhaled into the lungs [15].

Figure 2 (a) shows the Duke thorax model, with the lungs highlighted, while Fig. 2 (b) illustrates the number of lung cells in each horizontal section of the human body, as a function of the height from the feet. In particular, the figure reports the number of lung cells in the model representing the resting state (RS); i.e., the original model, and in the two realized models, the tidal breath (TB) and the deep breath (DB), respectively.

From the figure, an overall view of the levels where the lung expansion occurred is obtained. In particular, it can be noted that the rib cage expansion in the TB and DB models follows the behavior of the RS model in the higher sections (from 140 cm to 150 cm in Fig. 2 (b)). Then the expansion becomes more irregular; this is due to the drop in the diaphragm of 2 cm and 4 cm for the TB model and DB model, respectively.

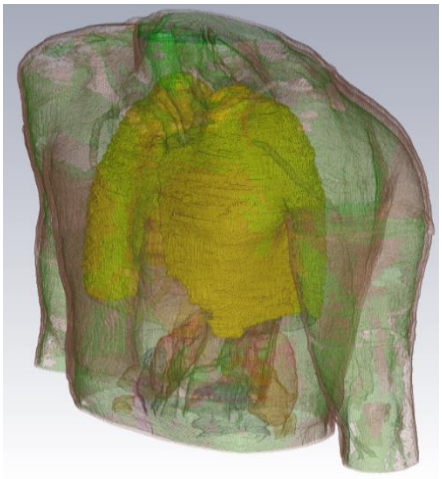

(a)

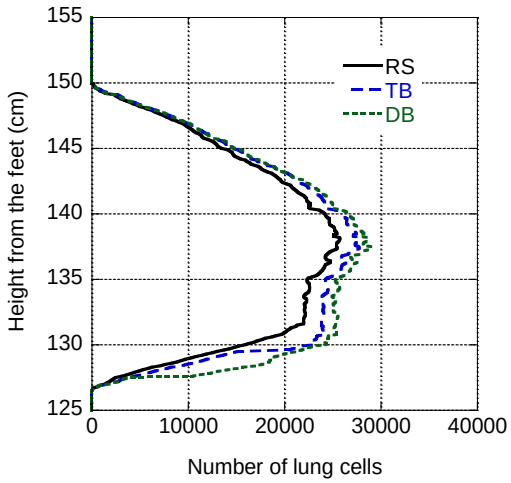

(b)

Fig. 2. (a) Thorax model of the Duke with lungs highligthed, and (b) number of lung cells in the transversal plane, for the RS, TB and DB models, as a function of the height from the feet.

The two new lung models have a final volume of 4262.171 cm^3 and 4530.206 cm^3, for TB and DB respectively, obtained from an initial volume of 3849.216 cm^3 (RS). Each model is made by 77 different tissues whose dielectric properties' values were obtained as a function of the frequency from the database available online at http://www.itis.ethz.ch/itis-for-health/tissueproperties/database/database-summary and based on data of Gabriel et al. [16].

In particular, the dielectric properties of the lung were assumed equal to that of inflated lung for the TB and DB models, and equal to the deflated lung for the RS model.

Moreover, the lung mass density was assumed equal to that of inflated lung (ρ_{LI} = 394 kg/m^3) in both TB and DB models, while for the RS model (man at the end of the expiration phase) an average value between the inflated lung (ρ_{LI}) and deflated lung mass density (ρ_{LD} = 1050 kg/m^3) was used, in order to take into account that the lung is never totally deflated; i.e., there is always a certain percentage of air within it.

To insert the VH into the FDTD code, a spatial resolution of 2 mm was chosen between 1 GHz and 5 GHz, that was reduced to 1 mm between 6 GHz and 9 GHz. On the other hand, for the Duke models, a 1 mm resolution was used at all frequencies. At the highest frequency of interest (9 GHz), the 1 mm resolution corresponds to less than 1/5 of the wavelength for all body tissues and is almost equal to 1/10 of the penetration depth of the electromagnetic field, thus allowing a good approximation of the spatial variations of the electromagnetic field [17].

III. RESULTS

A. Validation

Table 1 reports the RCS of the human body obtained from literature data, both experimental [2], [4]-[5] and numerical [1], [6]-[7]. In particular, in [6] and [7] the human body model considered is the Visible Human, while in [1] a scaled version (i.e., a thinner version) of the Visible Human was studied. The reported data indicates that, in the considered frequency range, RCS absolute values show large fluctuations with frequency and with the anatomical model considered, with values between 0.01 m^2 and 6.3 m^2. In particular, these variations can be attributed to the positioning and shape of the various sub-scatterers on which each considered subject can be divided [6].

In order to validate the numerical procedure, the RCS of the VH was studied between 1 and 9 GHz and compared with the data reported in [6]. In these simulations, the dielectric properties of tissues were varied with the frequency according to [16].

Figure 3 shows the backward RCS; i.e., the RCS obtained for $\theta = 90°$ and $\varphi = 270°$ (see Fig. 1).

From the figure a good agreement with [6] is obtained, with differences within 20% up to 7 GHz. At 8 GHz a very high value is obtained in [6], which seems to be out-side the trend of the other data.

It must be noted here that, in [6] a cell resolution of 2 mm was used for all the considered frequencies, even if, at the highest frequencies considered, such values are higher than the standard used criteria for FDTD stability and accuracy.

Furthermore, it is worth noting that similar discrepancies in the RCS results were also obtained in [7], where the RCS was computed, for the same human body model, by using two different numerical codes; i.e., FDTD and Xpatch.

Table 1: Literature data

	RCS (m^2) Experimental Results			RCS (m^2) Numerical Results		
f (GHz)	Shultz [2]	Bernardi [4]	Piuzzi [5]	Dogaru [6]	Dogaru [7]	Pisa [1]
0.40	1.12					
0.50						1.00
1.00		0.45	0.46	0.01	1.58	0.60
1.10	0.88					
1.50			0.11			0.90
2.00		0.26	0.03	0.19	0.32	1.00
2.40						
2.50			0.03			
2.80	0.49					
3.00		0.25	0.05	0.79	3.16	
3.50						
4.00		0.27	0.02	0.39	1.00	
4.50			0.15			
4.80	1.74					
5.00		0.29	0.18	1.00	1.00	
5.50			0.07			
6.00		0.24	0.06	0.10	6.31	
6.50						
7.00		0.2	0.03	0.25		
7.50			0.04			
8.00		0.23	0.06	1.26		
8.50			0.03			
9.00		0.25	0.01	0.10		
9.40	1.00					
9.50			0.02			
10.0		0.4	0.03			

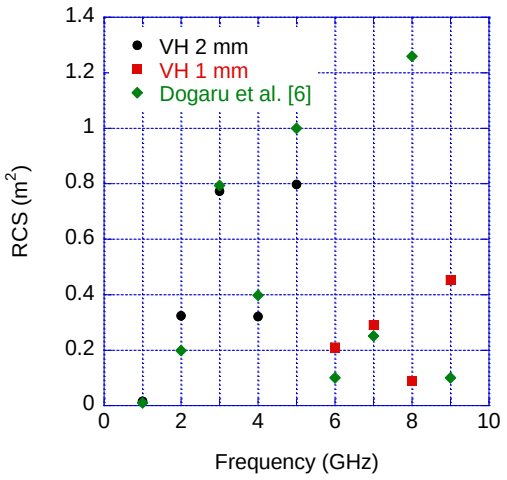

Fig. 3. Comparison between the Visible Human results and RCS values reported in [6].

B. Duke RS model

The Duke anatomical model in the resting state condition was then considered. The Duke RCS was evaluated with 1-degree resolution. Figure 4 shows the RCS at the frequency of 3 GHz as a function of the azimuth (φ). A persistent feature of the RCS is the strong value from the back of the body (φ = 90°), while lower values are obtained along the other directions.

Figure 5 shows the RCS for the Duke RS model as a function of the frequency in the xy plane along the propagation direction; i.e., for θ = 90° and φ = 270°. In the figure, the RCS values previously obtained from the Visible Human (Fig. 3) are also reported for comparison purposes. From the figure, the great variability of the RCS is evident (see also Table 1): it shows an oscillating behavior with peaks and valleys depending both on the frequency and on body models. In particular, with reference to the body models it can be noted that the VH is 1.80 m tall and weighs 105 kg, while the Duke is 1.77 m tall and weighs 72.4 kg.

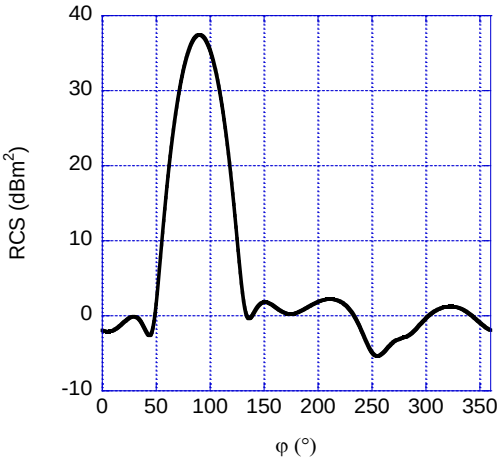

Fig. 4. RCS in the xy plane (θ = 90°) as a function of φ.

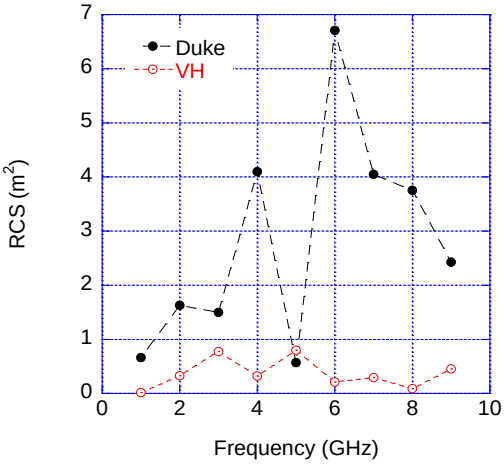

Fig. 5. RCS as a function of the frequency in the xy plane at φ = 270°.

C. Breath anatomical model results

Exploiting the TB and DB models described in Section II.B, simulations were conducted sweeping the frequency in the 1 GHz - 9 GHz range, with 1 GHz step.

Figure 6 shows the RCS obtained for the three developed models in the direction of the incident plane wave (θ =90°; φ = 270°). Observing the data, the RCS values are different for the three models, suggesting that the RCS changes during respiration and that this change varies with the frequency.

To interpret the obtained results, it can be noted that the three models have a different geometry both of the lungs and of the external surface, due to the rib cage enlargement and to the drop of the position of the diaphragm during respiration. Moreover, also the lung tissue characteristics change among the three models, both with reference to the dielectric properties and to the lung mass density, as previously detailed. It is worth mentioning that a similar result, i.e., an oscillating behavior of the RCS values, was also obtained experimentally in [5], for the end-inspiration and end-expiration breathing phases.

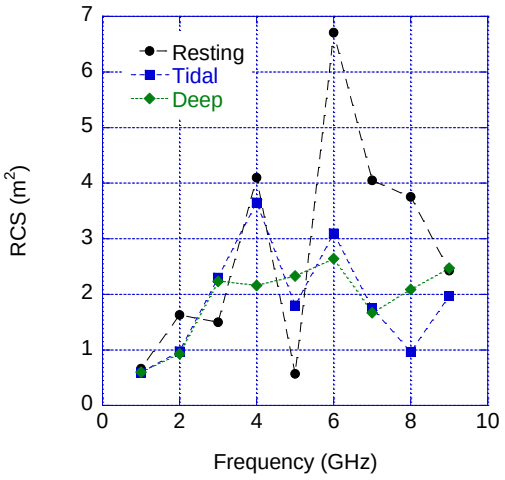

Fig. 6. RCS for the resting state, tidal breath, and deep breath models for theta = 90° and φ = 270°.

D. Homogeneous model

To understand if the results of the previous section are conditioned by the geometry rather than by the dielectric parameter differences, a homogeneous man model was considered.

In particular, the TB model was simulated substituting all the 77 tissues with the skin dielectric parameters at each computed frequency. Obtained RCS results for the homogeneous tidal breath (HTB) model are shown in Fig. 7 compared with those of the non-homogeneous TB model.

Results show differences between the HTB and the TB models, less evident at high frequencies where, due to superficial absorption of the field, the homogeneous skin

model behaves like the inhomogeneous one. Moreover, it is interesting to note that low differences between TB and HTB are obtained at low frequencies also, where probably the different dimensions of the thorax due to the different lung geometries influence most the electromagnetic reflection process.

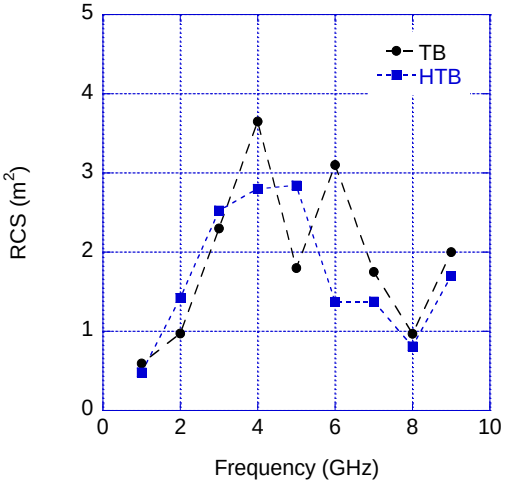

Fig. 7. Comparison between the tidal breath Duke model and the homogeneous tidal break Duke model.

IV. CONCLUSION

The knowledge of the RCS of the human body is of vital importance in the development of UWB radar for the remote detection of the respiratory activity. In fact, these radars rely on the electromagnetic field scattered by the human body towards the receiving antenna. Several studies were devoted to the evaluation of the human body RCS, finding very different results, so that it is very difficult to obtain a general rule to be used in UWB radar design. Moreover, the published studies considered resting state human body; i.e., bodies at the end of the respiration, when the lungs are almost empty.

In this paper, the RCS values of breathing subjects as a function of frequency were evaluated in the 1-9 GHz frequency band using a self-developed numerical code. In particular, three phases of the respiration activity were considered: resting state, tidal breath and deep breath. The three human body models had different geometries, both of the lungs and of the surrounding thorax, as well as different dielectric properties values to represent the different states of the lungs; i.e., empty (RS), partially filled with air (TB), almost completely filled with air (DB).

Obtained RCS absolute values for the resting model showed large fluctuations with the frequency, with values between 0.5 m^2 and 6.7 m^2 in agreement with the literature. With reference to breathing subjects, it was shown that the RCS changes between the three considered models, and that the entity of this change depends on the frequency.

In order to understand if the computed results were more influenced by the different geometries of the thorax or by the dielectric parameters, a homogeneous tidal breath model was considered. Results showed that RCS changes are due both to the different anatomy between the two models and to the differences in tissues dielectric parameters; in particular, the dielectric properties values seem responsible for most of the differences obtained in the frequency range between 4 and 6 GHz.

It is worth noting that the obtained behavior of the RCS with the frequency can be understood observing that the RCS of the human body is influenced by resonances of the various body segments. Therefore, small variations of the body geometry and of the tissue dielectric properties have a strong influence on the RCS values.

REFERENCES

[1] S. Pisa, P. Bernardi, M. Cavagnaro, E. Pittella, and E. Piuzzi, "A circuit model of an ultra wideband impulse radar system for breath-activity monitoring," *Int. J. Num. Model.*, vol. 25, no. 1, pp. 46-63, 2012.

[2] F. V. Schultz, R. C. Burgener, and S. King, "Measurement of the radar cross section of a man," *Proc. IRE*, vol. 46, no. 2, pp. 476-481, Feb. 1958.

[3] J. E. Kiriazi, O. Boric-Lubecke, and V. M. Lubecke, "Dual-frequency technique for assessment of cardiopulmonary effective RCS and displacement," *IEEE Sensors J.*, vol. 12, no. 3, pp. 574,582, Mar. 2012.

[4] P. Bernardi, R. Cicchetti, S. Pisa, E. Pittella, E. Piuzzi, and O. Testa, "Design, realization, and test of a UWB radar sensor for breath activity monitoring," *IEEE Sensors J.*, vol. 14, no. 2, pp. 584-596, Feb. 2014.

[5] E. Piuzzi, P. D'Atanasio, S. Pisa, E. Pittella, and A. Zambotti, "Complex radar cross section measurements of the human body for breath activity monitoring applications," *IEEE Trans. Instrum. Meas.*, vol. 64, no. 8, pp. 2247-2258, Aug. 2015.

[6] T. Dogaru, L. Nguyen, and C. Le, "Computer models of the human body signature for sensing through the wall radar applications," *ARL-TR-4290*, Adelphi, MD: U.S. Army Research Laboratory, 2007.

[7] T. Dogaru and C. Le, "Validation of Xpatch computer models for human body radar signature," *ARL-TR-4403*, Mar. 2008.

[8] M. Cavagnaro, S. Pisa, and E. Pittella, "Anatomical models of breathing subjects for absorption and scattering analysis," *EMC Europe 2013*, Sept. 2013.

[9] M. Cavagnaro, E. Pittella, and S. Pisa, "Evaluation of the electromagnetic power absorption in humans exposed to plane waves: the effect of breathing activity," *Int. J. Ant. Prop.*, vol. 2013, Article ID 854901, 7 pages, 2013.

[10] K. S. Nikita, M. Cavagnaro, P. Bernardi, N. K.

Uzunoglu, S. Pisa, E. Piuzzi, J. N. Sahalos, G. I. Krikelas, J. A. Vaul, P. S. Excell, G. Cerri, S. Chiarandini, R. De Leo, and P. Russo, "A study of uncertainties in modeling antenna performance and power absorption in the head of a cellular phone user," *IEEE Trans. Microw. Theory Techn.*, vol. 48, no. 12, pp. 2676-2685, 2000.

[11] K. S. Kunz and R. J. Luebbers, *The Finite Difference Time Domain Method for Electromagnetics*, CRC Press, Boca Raton, FL, USA, 1993.

[12] A. Taflove, *Computational Electrodynamics: The Finite-Difference Time-Domain Method*, Artech House, Norwood, MA, USA, 1995.

[13] M. J. Ackerman, "The visible human project," *Proceedings of the IEEE*, vol. 86, no. 3, pp. 504, 511, Mar. 1998.

[14] A. Christ, W. Kainz, E. G. Hahn, et al., "The virtual family—development of surface-based anatomical models of two adults and two children for dosimetric simulations," *Phys. Med. Biol.*, vol. 55, no. 2, pp. N23-N38, 2010.

[15] E. N. Marieb and K. Hoehn, *Human Anatomy & Physiology*, Pearson International Edition, 2007.

[16] S. Gabriel, R. W. Lau, and C. Gabriel, "The dielectric properties of biological tissues: III. parametric models for the dielectric spectrum of tissues," *Phys. Med. Biol.*, vol. 41, pp. 2271-2293, 1996.

[17] P. Bernardi, M. Cavagnaro, S. Pisa, and E. Piuzzi, "SAR distribution and temperature increase in an anatomical model of the human eye exposed to the field radiated by the user antenna in a wireless LAN," *IEEE Trans. Microw. Theory Techn.*, vol. 46, no. 12, pp. 2074-2082, Dec. 1998.

Marta Cavagnaro received the Electronic Engineering degree (cum laude) and the Ph.D. degrees from Sapienza University of Rome, Rome, Italy, in 1993 and 1997, respectively. From 2000 to 2012, she was Assistant Professor at the Dept. of Electronic Engineering, Sapienza University of Rome. Presently she is Associate Professor at the Department of Information Engineering, Electronics and Telecommunications of the same university. Her research interests are related to dosimetric aspects of the interaction between EM fields and biological systems, medical applications of EM fields, environmental impact of mobile communication systems, and numerical techniques in electromagnetics. She is author or co-author of more than 120 scientific papers, and serves as Reviewer for several scientific journals.

Erika Pittella received the M.S. (cum laude) and Ph.D. degrees in Electronic Engineering from Sapienza University of Rome, Rome, Italy, in 2006 and 2011, respectively. She is currently a Research Associate with the Dept. of Information Engineering, Electronics and Telecommunications, Sapienza University of Rome. Her main research activities are related to the modeling of UWB radars for the remote monitoring of cardio-respiratory activity and to the design of sources, antennas, and receivers of such systems. Her research interests also include dosimetric aspects of the interaction between electromagnetic fields radiated by UWB radar systems and exposed subjects.

Stefano Pisa (M'91) received the Electronic Engineering and Ph.D. degrees from Sapienza University of Rome, Italy, in 1985 and 1988, respectively. In 1989, he joined the Dept. of Information Engineering, Electronics and Telecommunications as a Researcher. Since 2001, he has been an Associate Professor with the same university. His research interests are the interaction between EM fields and biological systems, therapeutic and diagnostic applications of EM fields, and the modeling and design of MW circuits. He has authored over 150 scientific papers and numerous invited presentations. He serves as a Reviewer for different international journals. He is currently "Consulting Member" of the "Scientific Committee on Physics and Engineering" of the ICNIRP and a Member of the Advisory Group of the Dutch project "Electromagnetic Fields and Health".